Solar RRL
www.solar-rrl.com

Unveiling the Potential of Ultraviolet Fluorescence Imaging as a Versatile Inspection Tool: Insights from Extensive Photovoltaic Module Inspections in Multi-MWp Photovoltaic Power Stations

Claudia Buerhop-Lutz, Oleksandr Stroyuk,* Oleksandr Mashkov, Jens A. Hauch, and Ian Marius Peters*

UV fluorescence imaging (UVF) has the potential to grow into a powerful, informative, and economically attractive inspection method for photovoltaic (PV) power stations. UVF demonstrates the ability to indicate differences in polymer types and degradation states in backsheets and encapsulation materials of PV modules. The data acquisition rate of UVF measurements is 10 to 15 times higher than that achieved by state-of-the-art near-infrared spectroscopy, enabling the mapping of the bill of materials (BoMs) and degradation state for every module in large PV arrays. Combinations of UVF with vibrational spectroscopies allow the polymer BoMs to be recognized and correlated with aging phenomena such as metal corrosion or potential induced degradation. UVF imaging can also be used for conventional visualization of nonmaterial-related anomalies, such as hot cells or cell cracks. The low purchase cost of the equipment makes UVF an affordable and high-throughput diagnostic method yielding comprehensive information that would otherwise only be accessible by combining several slower and more laborious methods. Automated UVF image analysis and refinements of correlations between different BoMs and UVF pattern geometry can further unlock the potential of UVF as a straightforward tool accessible to all stakeholders and promote proactive strategies for the optimization of the reliability and performance of PV power stations.

1. Introduction

Regular inspections of solar parks are mandatory and common practice to ensure safe and efficient operation. However, in recent years, operating problems have increasingly been observed in solar parks due to the unexpected premature degradation of polymer components in photovoltaic (PV) modules, in particular, encapsulants and backsheets.[1–4] It is now understood that ethylene-vinyl acetate (EVA) copolymer, a common encapsulant in PV modules, suffers from photochemical degradation leading to the formation of acetic acid.[4–6] This degradation process, when combined with external factors such as oxygen and moisture, results in the deterioration of the backsheet material.[1,6]

The solar industry, including operators and technicians, was unprepared for the challenges posed by polymer degradation. There is a lack of expertise, experience, and appropriate equipment for testing and evaluation. The implications of highly degraded polymers are severe, and inverters may fail to connect to the grid due to backsheet-driven insulation problems,[4,7–9] leading to an inability to feed electricity into the grid and consequent income losses for solar park owners or module failures such as potential-induced degradation (PID).[4,10]

Currently, the standard procedure to address this issue involves dismantling and transporting individual PV modules to test laboratories for characterization through multiple methods, such as measurements of current–voltage (IV) curves under standard test conditions (STC), electroluminescence (EL) imaging, "wet leakage" test, and nondestructive characterization of the backsheet air layer using Fourier-transform infrared (FTIR) or Raman spectroscopy.[11,12] However, this approach raises several concerns. First, the selection and number of representative PV modules for lab characterization may not adequately reflect the overall distribution of the bill of material (BoM) of the solar park. Second, laboratory tests may not accurately mimic the complex operating conditions experienced in the field. Third, the interaction and dependencies between healthy and degraded PV modules within an electrical circuit or string are not captured by lab tests. Fourth, multilayer backsheets and EVA encapsulants cannot be analyzed in detail.

C. Buerhop-Lutz, O. Stroyuk, O. Mashkov, J. A. Hauch, I. M. Peters
Forschungszentrum Jülich GmbH
Helmholtz-Institut Erlangen Nürnberg für Erneuerbare Energien (HI ERN)
91058 Erlangen, Germany
E-mail: c.buerhop-lutz@fz-juelich.de; o.stroyuk@fz-juelich.de

The ORCID identification number(s) for the author(s) of this article can be found under https://doi.org/10.1002/solr.202400566.

DOI: 10.1002/solr.202400566

To our understanding, laboratory tests do not effectively capture the relationship between system performance at real operating conditions and material properties. This has led to a search for field-ready alternatives to the labor-, time-, and cost-consuming, lab-based module characterizations, allowing for nondestructive and noninvasive outdoor characterization of field-aged PV modules. The scarcity of such approaches for field analysis of polymer BoMs is one of the reasons for the currently limited knowledge of field degradation mechanisms.[9,11–13] Polymer degradation can cause severe reliability and performance issues that are not indicated by standard inspection techniques such as infrared (IR)[14–16] or EL imaging,[17] as well as photoluminescence imaging.[18,19] These issues often become apparent in monitoring data only when there is already a significant negative impact on the performance, while suitable data such as ground impedance are measured but not logged by inverters.

Currently, the industry reacts to problems as they occur. However, proactive measures would be far more effective, allowing operators to anticipate and mitigate issues before they impact performance. In this context, UV fluorescence imaging (UVF)[20–22] emerges as a potentially revolutionary method for the characterization of the health of PV modules in the field. When supported by appropriate spectral and electrical measurements, UVF imaging offers diverse and comprehensive information about the condition of the PV modules, showing many unique strengths and high effectiveness. Being simple and cost-effective, this technique also provides unparalleled insights that are crucial for maintaining the reliability and performance of solar parks, for example, location of specific PV modules of interest. It stands out as a promising tool that could strengthen traditional/standard methods, enabling proactive maintenance and ensuring the long-term efficiency of PV installations. The present perspective aims to highlight the potential of UVF imaging, both in conventional measurements, such as crack detection, and in novel applications going beyond the current state-of-the-art, such as the identification of BoM and degradation status of polymer components of PV modules made possible due to a combination of UVF imaging with spectral polymer analysis by vibrational spectroscopies.

2. UVF Imaging—Diverse and Comprehensive Inspection Tool

Night-time exploration of a solar park, armed with UV lamps and cameras, provides an exciting and scientifically relevant experience, showing features that remain hidden for daylight inspections. After collecting UVF images of many thousands of modules in several PV power stations, an observer develops an ability to visually recognize different UVF patterns associated with specific polymer BoMs and the intricate structures of cell cracks contrasted by UVF patterns. A later and deeper analysis of subtle features of UVF patterns allows additional meaningful information to be extracted, for example, variances in junction box types or systematic cell cracks reflecting maintenance-induced damages of PV modules.

2.1. UVF Imaging—a Tool That Gives Deep Insight into Module Degradation

UVF images were recognized as a rich source of multiple data on both polymer BoMs and the degradation modes of PV modules. **Figure 1** Illustrates the diversity of UVF patterns, showcasing examples of anomalies and changes that stand out in the regular structures. These observations include variations in the backsheet materials and EVA encapsulant properties, showing clear differences in their degradation patterns. Additionally, variations in the fluorescence intensity within the UVF patterns of EVA encapsulants indicate different levels of photochemical degradation, which can potentially impact the overall reliability and performance of the PV module.

Cell cracks are another critical issue routinely revealed by UVF imaging. The intricate structures of cell cracks are developed

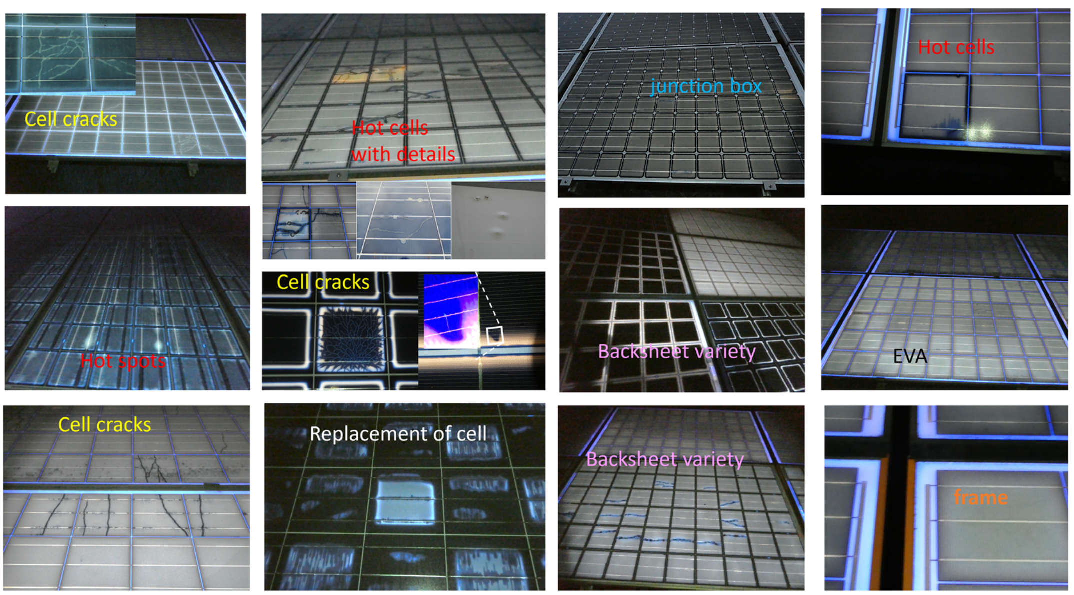

Figure 1. Exemplary UVF images, displaying a variety of observations and findings.

through competing processes of UVF formation and oxidative quenching, allowing for simple quantification of cell crack type,[23,24] distribution, and frequency. Local phenomena such as hot cells and hot spots can also be identified, indicating localized issues that may lead to further degradation if left unattended.

Furthermore, UVF imaging detects differences in junction box types, providing insights into the compatibility and reliability of various designs. Delamination, which is the separation of layers within the module, leading to moisture ingress and further degradation, can be observed in UVF images. Issues with the module frame and any material patches applied for repairs can also be assessed for their impact on module integrity.

These capabilities of UVF imaging can be exemplified by a case field study where we collected UVF imagery on more than ≈20.000 PV modules at several PV power stations in various climatic conditions complementing UVF imaging with visual failure detection (VIS), near-infrared absorption (NIRA) spectroscopy, and IR and EL imaging (**Table 1**). The visual inspection was focused on marking visual anomalies in cells (cracks, hot cells, snail trails, etc.), polymers (delaminations, discoloration, etc.), and corrosion of metal components. Many of these instances were also identified in IR and EL imagery. NIRA spectroscopy revealed BoM and the degradation status of polymers.

Table 1 shows that, unlike other methods, UVF imaging can provide meaningful information on each and any of the tested parameters, detecting failures in cells, metal interconnects, and polymers, as well as providing identification of BoM when properly calibrated using the NIRA database (see details below). When compared to other tools of field inspection taken alone, UVF imaging revealed an unparalleled versatility and level of insights, strongly enhancing the field analysis of the health of PV modules.

2.2. UVF Imaging—BoM-Related Findings

UVF imaging is a convincing and inspiring inspection tool, as it provides comprehensive information in every single recording/picture recorded in the field done in the real environment.[25–27] The immediate eye-catching topic is the BoM-related differences in UVF images. The use of different polymers, encapsulants, and backsheets, in PV module production results in distinctive, material-specific UVF patterns developed after field aging of PV modules. These patterns show multiple variations in UVF emission intensity, shape, and width of the cell edge structures. However, though being noticed in earlier reports, the exact relationships between specific UVF patterns and particular BoMs remained missing because the BoM of field-exposed modules is in general unknown and requires an independent tool to be identified and then related to the geometry of UVF patterns. The proof of concept of such an approach was performed by combining UVF imaging with BoM identification using NIRA spectroscopy,[28] discussed in detail below.

The heterogeneity of UVF patterns has revealed multiple BoMs in numerous inspected and reported PV power stations, even among PV modules from the same manufacturer and brand. The high variance in the materials used by module manufacturers appeared to be standard practice but is often unexpected and surprising for field operators. **Figure 2**a illustrates an exemplary collection of different UVF patterns observed for different backsheet types. We classified these patterns into three classes with patterns showing the homogeneous distribution of UVF intensity across the cell area designated as Class I, patterns with UVF intensity accumulated near the edges showing square/ring-shaped structures united in Class II, and patterns with low UVF intensity across the cell area but high intensity between the cells (stemming from backsheet) denoted as Class III.

The pristine PV modules show no UVF emission (see photographs in Figure 2b, cases Ia, b). The modules exposed to solar irradiation undergo photochemical transformations generating acetic acid (HAc) and fluorescing species in the frontal EVA layer. The shape of the UVF pattern depends on additives present in the EVA matrix. With no UV absorbers present, the UVF intensity is distributed homogeneously across the UVF pattern, which mimics the underlying Si cell (case IIa). In the presence of UV absorbers that can migrate in the EVA matrix[29] forming depleted edge areas, frame-like UVF patterns are observed (case IIb).

Photogenerated HAc penetrated the backsheet resulting in the hydrolytic degradation of backsheet components allowing more air oxygen inside the module that partially oxidizes fluorescent species in EVA and quenches UVF emission. As a result, the area of square/ring-shaped UVF patterns gradually decreases (case IIIa), while the frame-like patterns shrink and move from the Si cell edges to the center of the cells (case IIIb).

Table 1. Comparison of findings using UVF imaging with other optical methods and findings in six solar parks. Explanation of markers: "x"—detectable, "(x)"—at certain circumstances detectable, "?"—not known; numbers: quantity of different classes per PV power station, percentages: fraction of affected PV modules.

Findings		Methods					PV power stations					
		UVF	NIRA	IR	EL	VIS	A	B	C	D	E	F
BoM	Frame	X	–	–	–	–	1	1	2	1	1	1
	Substitutions (cells, EVA patches)	X	–	–	–	–	0%	0.02%	0.1%	0.06%	0%	0%
	Junction box	X	–	–	–	x	1	?	2	1	2	1
Polymers	Differences in backsheet EVA	X	x	–	–	(x)	3	4	4	4	5	3
	Degradation	(x)	x	–	–	–	–	–	–	–	–	–
Failures	Cell cracks	X	–	(x)	x	(x)	?	60%	80%	83%	79%	69%
	Hot cells	X	–	x	–	(x)	0%	0.18%	0.14%	0.09%	0.14%	0.10%
	Others: e.g., PID, corrosion, delamination	(x)	–	x	x	x	0	10%	0	5%	15%	4%

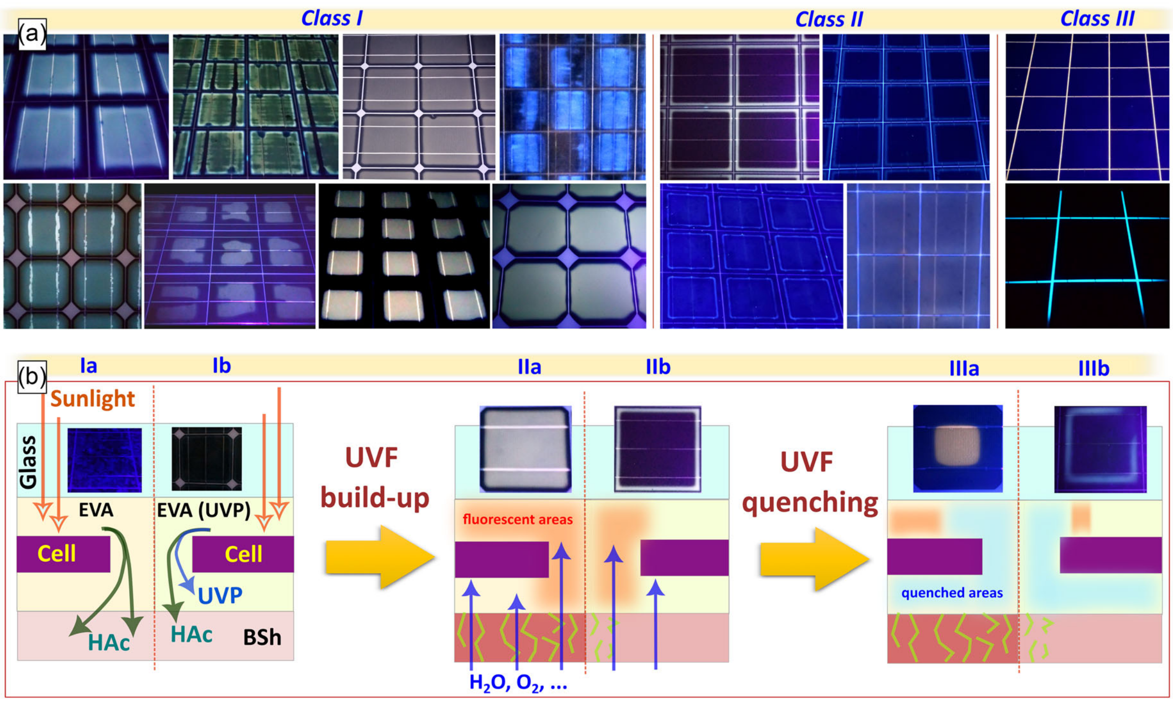

Figure 2. a) Exemplary UVF images collected for PV modules with different backsheet classes. b) Schematic illustration of primary photoinduced degradation and secondary oxidative degradation of polymer components of PV modules resulting in the formation of characteristic UVF patterns.[5] UVP stands for a UV-protecting additive.

By combining UVF imaging with near-infrared absorption (NIRA) spectroscopy and forming a comprehensive BoM database, various UVF patterns can be analyzed nondestructively and associated with specific materials. At that, NIRA enables the noninvasive analysis of all layers within multilayer backsheets,[25,28,30] provided a reference exists in the database. The principle of the method is illustrated in **Figure 3** for an exemplary set of four backsheet types with the composition of backsheet components (Figure 3a) identified independently by cross-sectional Raman microscopy.[25]

The UVF images of these backsheet types (Figure 3b) show clear distinctions in pattern geometry which can be translated into UVF intensity profiles (red lines in Figure 3b) and subjected to principal component analysis (PCA). The PCA yields distinct clusters for each of the backsheet types (Figure 3c) allowing the latter to be deduced solely from the UVF image provided this backsheet type is present in the database. The quality of clustering is similar to that obtained by analyzing NIRA spectra (Figure 3d).[21] However, the UVF-imaging-based backsheet identification appears to be an order of magnitude faster than spectroscopic analysis.[26]

With this approach to backsheet identification being so fast, UVF imaging can be used independently to map BoMs over hundreds and thousands of PV modules at field inspection. **Figure 4** illustrates the variety of polymer materials in a single row and a map of backsheet types identified in a section of a multi-MWp PV power station. The formation of two PA clusters aligns with one PA cluster having corrosion, and the other not. Such extensive mapping by NIRA-supported UVF coupled with simultaneous visual inspection provides a unique ability to correlate visual anomalies (corrosion, delamination, cracks, etc.) with specific BoMs.

Apart from the BoM identification, the combination of NIRA with UVF offers information on the aging and degradation status of the EVA encapsulant. Spectral NIRA measurements show the content of carbonyl groups resulting from the oxidative degradation of the polymer as well as water content, which can be quantitatively expressed as a carbonyl index (CI) and water index (WI) and used to compare the depth of oxidative degradation for different module types, climates, and plant ages.

We found that different polymer combinations show different signs and dynamics of degradation at different locations,[26] leading to variations in CI and WI values depending on the materials used and local conditions. We could correlate CI and WI values with anomalies and failures identified through other methods, like IR or VIS, and link the findings to specific UVF patterns and BoMs.

An example shown in **Figure 5** demonstrates three UVF patterns correlated to three polymer combinations (three EVA types, one backsheet type), as well as particular signs of degradation (corrosion) and failure (formation of PID). There is a clear trend with higher CI values corresponding to higher WI values. The higher degree of oxidative degradation negatively impacts the insulation resistance R_{iso} and leads to corrosion of metal interconnects. If R_{iso} values reach critically low levels, inverter issues arise, causing a loss of feed-in and revenue.[7,8]

Once the correlation between UVF pattern and possible implications for PV module reliability and performance is understood, UVF imaging enables upscaling, for example, the evolution from

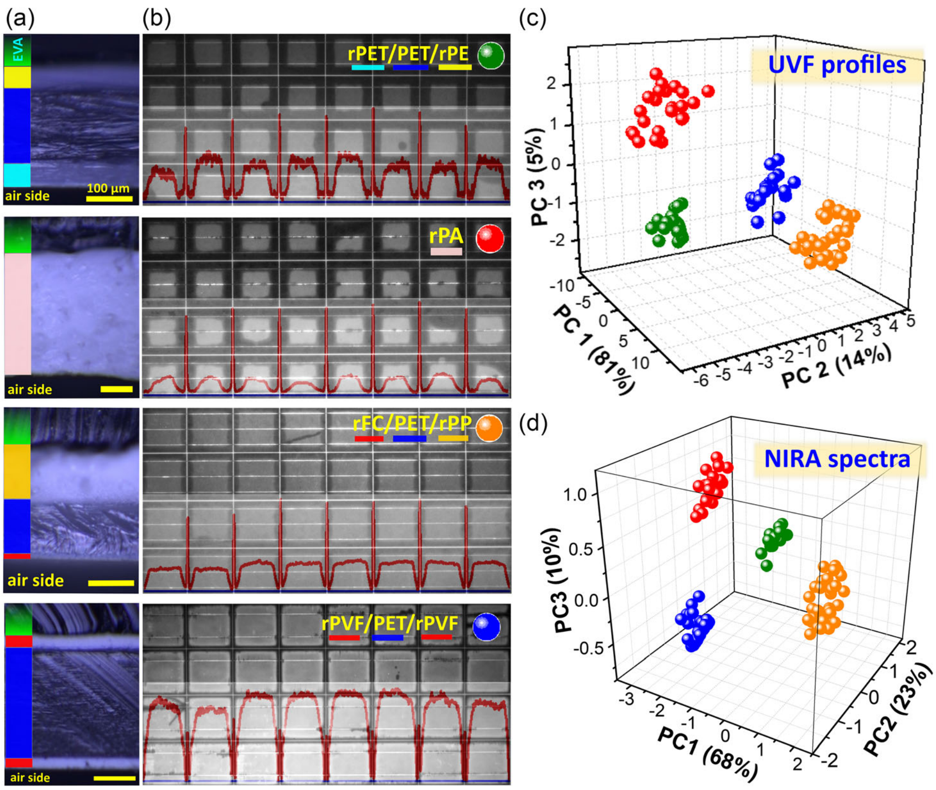

Figure 3. Backsheet identification from UVF images: a) Cross-sections of exemplary backsheets; b) UVF images and UVF intensity profiles of corresponding PV modules; c,d) PCA plots for four selected backsheet types produced for c) UVF intensity profiles and d) NIRA spectra. Abbreviations in the figure: PE—polyethylene, PET—PE terephthalate, r—rutile titania, PA—polyamide, PP—polypropylene, PVF—polyvinyl fluoride.

NIRA-based backsheet identification from a limited but representative number of PV modules to a UVF-imaging driven inspection of a much larger section of a PV system. In this upscaled mode, UVF imagery can become instrumental in localizing and mapping.[31] Critical modules and strings that pose a high risk of inverter shutoffs.

UVF imaging also reveals inhomogeneities across the PV module area, as illustrated in Figure 1 (example marked by EVA), where the inner PV module area is darker, indicating lower UVF intensity, probably due to an inhomogeneous temperature profile during the lamination process or uneven distribution of components in the raw materials of the EVA foils. While this remains speculative and challenging to clarify without destructive measurements, it is easy to spot and map through UVF imaging.

Additionally, UVF imaging can reveal variations in junction boxes. In a particular case study, we identified three types of junction boxes with different sizes for the single module manufacturer. The variations in UVF patterns can be explained by thermally induced changes in the adhesives or resins.

2.3. UVF Imaging—Non-BoM-Related Findings

In addition to the innovative identification of BoM-related patterns mentioned above, more conventional non-BoM-related UVF features are also important for a comprehensive analysis of a PV plant. These features (see examples in **Figure 6**a) can be detected across any material combination and constitute the major focus of most of the previous UVF imaging studies.

One prominent feature is the presence of cell cracks interrupting the regular UVF patterns of the PV modules (Figure 6b). According to our evaluation of more than 50 000 UVF images, on average 74% of the PV modules were found to exhibit crack structures, a finding consistent with Köntges' results.[32,33]

These cracks vary widely in type, including cracks under or near busbars, indents, perpendicular cracks to busbars, cracks around the corner, diagonal cracks, and multiple-branched cracks with varying frequencies.[23] The visibility and appearance of these cracks under UVF imaging are influenced by their age, as older cracks tend to have broader dark rims due to moisture and oxygen ingress increases. Comparative images in Figure 6b illustrate that UVF imaging can be as informative of the crack type and population as EL or PL imaging, at the same time being non-invasive (as compared to EL imaging) and much less demanding to the illumination power (in contrast to PL imaging).[34]

While determining the exact age of a crack is challenging and requires calibration for each material, distinguishing between fresh and old cracks based on UVF imaging is feasible.[35,36] The increased shadowing effect of older cracks helps in identifying their progression and potential impact on PV module performance.

Delamination features are particularly prominent in UVF images and vary depending on their location and origin. These can appear as dark and black or white and cloudy/milky

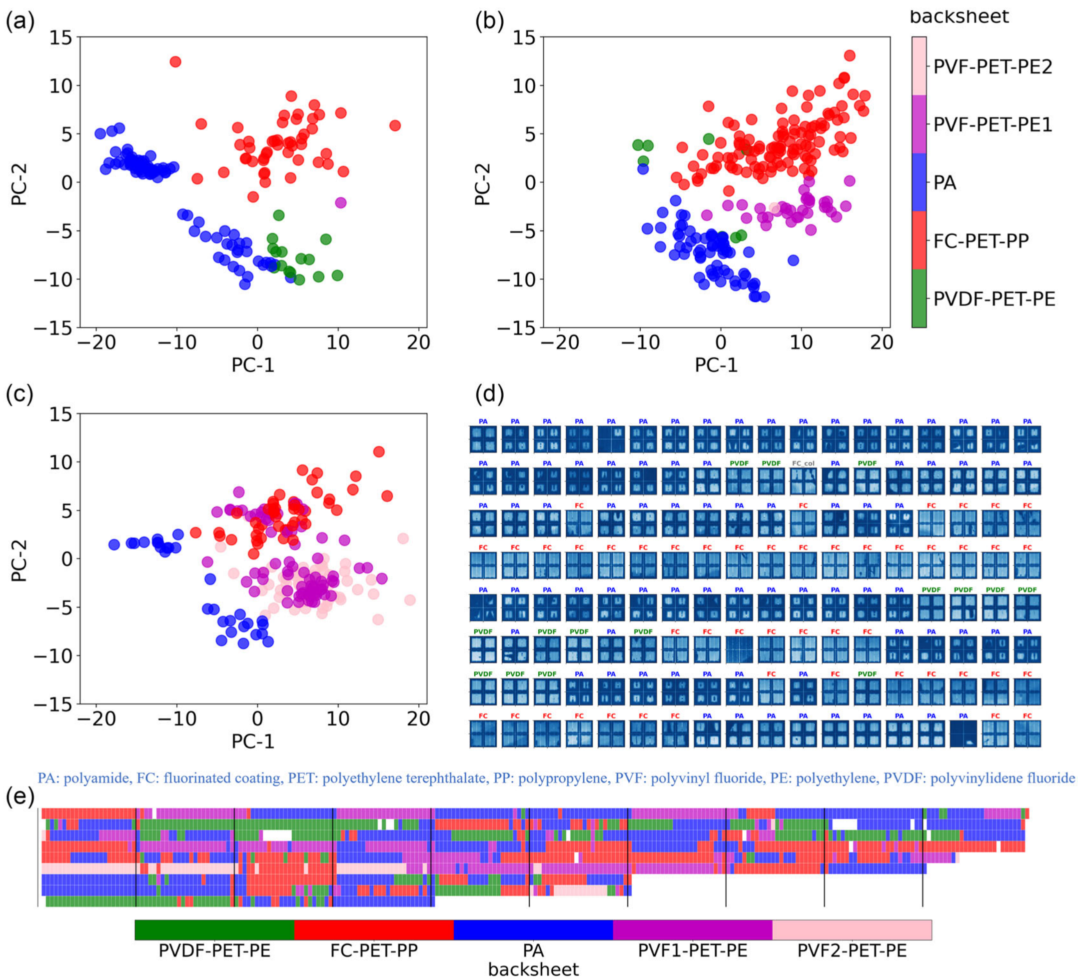

Figure 4. UVF imaging for backsheet classification, a–c) clustering of various backsheet types by principal component analysis for three rows for better visualization; d) visualization of cropped UVF images (2 × 2 cells), respectively backsheet distribution, for a single row with 144 PV modules (correspond to subfigure a); e) upscaling and mapping of backsheet type by combining UVF imaging and NIRA for a section of multi-MWp PV power station G (backsheet distribution of 1874 PV modules shown, ≈0.5 MWp). FC—fluorinated coating, PVDF—polyvinylidene fluoride.

areas. Black dendritic structures are observed along busbars and grid fingers, while irregular, "milky" white patterns indicate delamination between glass and EVA. Delamination between solar cells and EVA typically appears as dark areas. Although the implications on performance are not yet fully reported, the presence of delamination is a critical indicator of potential structural issues within the module.

UVF imaging also highlights very bright and intense patterns that correlate to hot cells and hot spots seen in IR imaging (Figure 6c). Our experience suggests that significant local temperature differences, well above $\Delta T >> 5$ K for a prolonged period, are required to produce these UVF signatures. This contrasts with temperature increases from bypassed substrings or PID, which do not exceed ΔT of 5 K and do not appear in UVF imagery.[14,37] **Table 2** quantifies the findings of heat-related failures, like string, substring, PID, and hot cells, detected by IR and UVF imaging. IR observations of the hot spots are rare with an average of 0.7% of modules with thermal anomalies, which corresponds to numbers presented by Jordan.[38]

UVF imaging identifies a minor fraction of the hot cell category linked to severe temperature increase and forced polymer degradation. Bright cells in UVF images often indicate severe failures, for example, soldering issues correlated with burn marks or cell cracking.

Unexpected UVF features include irregular local areas within a PV module, likely due to unplanned substitutions of cells or EVA patches that cause distinct UVF patterns. Additionally, variations in protective films deposited on frame material, as indicated in Figure 1, also produce unique UVF signatures. These variations can be due to manufacturing failures or later repairs, further highlighting the diverse applications of UVF imaging in detecting and diagnosing PV module issues.

2.4. UVF Imaging—Overview of Findings

Our field experience clearly shows that UVF imaging supported by reference spectral identifications of polymer BoM can provide diverse and comprehensive information giving new insights into

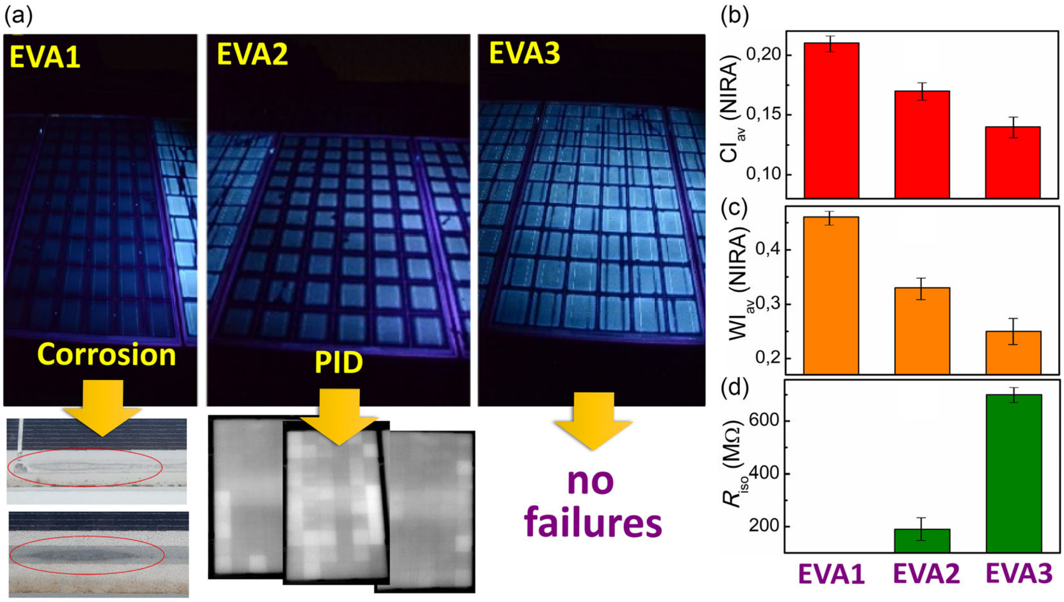

Figure 5. Different sorts of EVA for the same backsheet: a) representative UVF images of three different EVA sorts (EVA1, EVA2, and EVA3) found for the same PET/PET/PE backsheet and showing different failure modes, in particular, metal corrosion and PID (updated image[27]); b) average CI and c) WI derived from NIRA; and d) "wet" leakage insulation resistance R_{iso} of PV modules with the same backsheet and different EVA types.

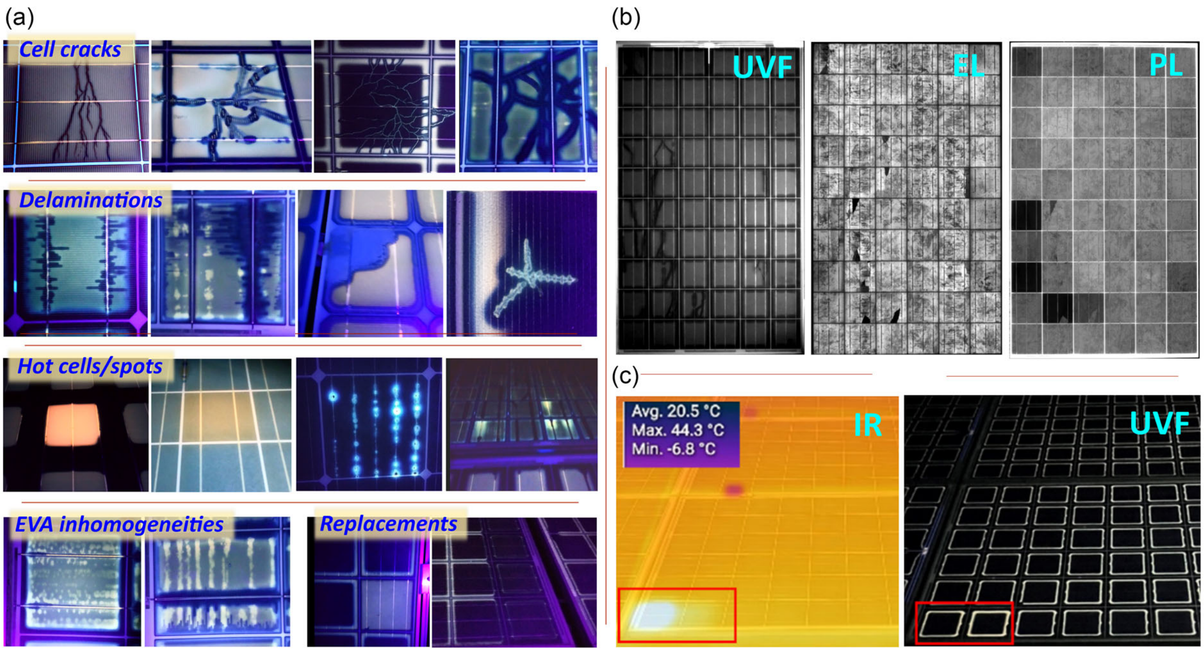

Figure 6. a) A collection of UVF images illustrating cell cracks, various cases of encapsulant delaminations, hot cells, hot spots, local inhomogeneities in EVA quality, and cases of cell/polymer replacements. Comparative sets of b) UVF, EL, and PL, and c) IR and UVF images taken from the same modules.

PV modules' health and aging. The key findings can be summarized as follows: 1) differences in polymers: UVF patterns influenced by EVA and backsheet materials allow for material identification; 2) inhomogeneities of EVA: anomalies suggest an inhomogeneous temperature profile during lamination; 3) degradation along busbars: observable features indicate degradation patterns along busbars; 4) cell cracks: distinguishing cracks with dark rims (moisture/oxygen penetration) and white cracks with unknown origin as well as crack age; 5) bright cells correlating with IR imaging: correlation with hot cells, potentially linked to hot spots; 6) variation of junction boxes: brightness differences likely tied to variations in heat transfer; 7) substitutions

Table 2. Comparison of findings and failures in IR and UVF imaging, fractions per module respectively strings.

Findings	PV power stations											
	A		B		C		D		E		F	
	IR	UVF	IR	UVF	IR	UVF	IR	UVF	IR	UVF	IR	UVF
Strings	0.72%	0%	0%	0%	0%	0%	0%	0%	0.48%	0%	0.42%	0%
Substring	0.08%	0%	0.08%	0%	0.22%	0%	0.18%	0%	0.40%	0%	0.53%	0%
PID	0%	0%	0%	0%	0%	0%	0%	0%	0%	0%	2.32%	0%
Hot cells, hot spot	0.29%	0%	0.37%	0.18%	0.30%	0.14%	1.22%	0.09%	0.60%	0.14%	8.71%	0.10%

of EVA patches or cells: identifiable through UV imaging; and 8) variations of frame material: observable differences in frame material characteristics.

2.5. UVF Imaging—Acquisition Rate/Cost

Among the methods routinely used for field inspections in PV plants, UVF imaging provides a uniquely favorable combination of the broad range of detected parameters, high acquisition rate, and low setup price. Even when realized as a manual human-driven procedure, UVF imaging can process 400–500 modules per hour per person requiring the lowest setup investments (see **Table 3**). Currently, this acquisition rate is dictated by the walking speed of the observed and camera acquisition time and is focused only on lower rows of PV modules. At that, UVF imaging provides BoM identification for all measured modules, which can be alternatively achieved by much slower NIRA measurements (25–35 modules per hour per person), the latter requiring high-end spectral equipment. Therefore, UVF imaging is 10–15 times faster than NIRA, making it a promising high-throughput characterization tool applicable for mapping the bill of materials and the degree of polymer degradation on large (multi-MWp) PV arrays.

IR and EL imaging provide only limited information on BoM-related issues and require flight permission over the PV plant (often being a problematic issue) and the participation of an electrician, respectively. Insulation resistance measurements are laborious as the electrical contacting of each string or module is required, whereby ≈75 strings (50 modules) can be measured per hour and person. Visual inspection appears as a simple but surprisingly efficient tool with multiple parameters detectable by a trained observer with a throughput rate of ≈300 modules, comparable to the efficiency of UVF imaging with no additional setup costs, making it a useful component of the multi-modal field inspection.[14,39]

3. Conclusion and Outlook

UVF imaging stands out as a powerful tool for inspections of PV modules in solar parks, offering unique capabilities either independently or in combination with other techniques to enrich and scale localized information to a broader, more representative sampling. UVF imaging delivers unparalleled insights into the bill of materials of PV modules and degradation features, distinguishing itself from conventional methods. In particular, based on reference near-infrared spectroscopy measurements, UVF imaging is capable of recognizing differences in the polymer components, that is, backsheet and encapsulation material. Being polymer selective, UV fluorescence imaging enables the correlation of different bill of materials with certain aging phenomena (e.g., metal corrosion) or module faults (e.g., potential induced degradation). **Figure 7** illustrates the unique features of UVF taken alone as well as in combination with other characterization tools.

In particular, UVF imaging enables accurate differentiation of materials within PV modules and localization of material variation across PV systems, facilitates the visualization of degradation features such as delamination, and highlights variation in frame material and localized substitutions (UVF unique). The outcomes of UVF imaging well correlate with IR and EL

Table 3. Evaluation of acquisition time for UVF in comparison with different inspection modes according to field experience of the HI ERN research group.

Method	Acquisition rate [module/h/person]	Setup price estimation (Euro)	Conditions/limitations
UVF	400–500	200–300	Limited by camera acquisition time and walking speed Only lower rows inspected
NIRA	25–35	≈20 000	Pairwise measurements (backsheet at rear side, EVA at front side) Limited by movements of a trolley to carry scientific measurement equipment
IR	20 000	5000+	Camera on a flying drone (flight permission required)
EL	250–350	1000+	Requires two persons during measurement and a presetup Number reported for a camera mounted on a stick
R_{iso}	10	4000+	Requires two persons during measurement and shutting off the modules
VIS	300	–	Pairwise inspection (backsheet at rear side, visual anomalies on front side) Limited by taking notes and walking speed

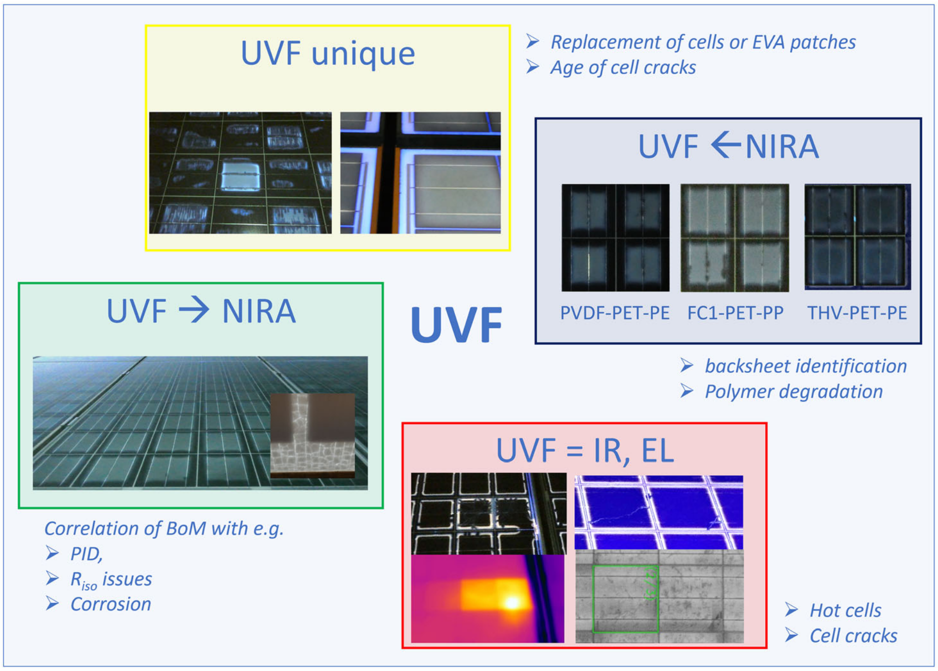

Figure 7. Strengths of UVF imaging alone and in combination with other exemplary techniques.

imaging (UVF = IR, EL) showing cell cracks and hot cells that impact module performance. Combining UVF imaging with spectral methods like NIRA, Raman, and FTIR allows specific UVF patterns to be correlated with specific backsheet types (UVF <-- NIRA) and degradation parameters (such as carbonyl and water indices). Finally, UVF imaging supports and explains observations from complementary methods (UVF --> other methods), for example, aimed at the analysis of PID and metal corrosion, linking them to specific material combinations.

The multidimensional data provided by UVF imaging enable the localization and mapping of specific information critical for efficient solar park maintenance. Applying robotics or drones for accelerated and automated data acquisition can further enhance its utility, particularly in large-scale PV installations. Enhanced identification of polymers based on spectral databases reduces the need for extensive lab tests, focusing instead on a select number of PV modules.

To fully unlock the potential of UVF imaging in solar park maintenance, further continued research is essential to deepen our understanding of UVF signatures in relation to backsheet and EVA combinations, emerging PV module technologies, and the effects of climate-induced aging. Automation and refinement of evaluation algorithms, coupled with the development of comprehensive databases, will contribute to the widespread acceptance and applicability of this simple yet highly informative method. These advancements will empower solar parks to adopt proactive strategies for optimizing the reliability and performance of PV power stations.

Acknowledgements

C.B.-L., O.S., O.M., J.A.H. and I.M.P. contributed equally to this work. This work is supported by the German Federal Ministry for Economic Affairs and Climate Action ("dig4morE", No. 03EE1090B; "PolymAERA", No. 03KN0053E), the Helmholtz Association in the framework of the innovation platform "Solar TAP" (No. 714-62150-3/1 (2023)), and Zentrales Innovationsprogramm Mittelstand (ZIM, project "RobInspec", No. 16KN083044) and co-funded by the European Union (ERC, C2C-PV, No. 101088359). Views and opinions expressed are however those of the author(s) only and do not necessarily reflect those of the European Union or the European Research Council. Neither the European Union nor the granting authority can be held responsible for them.

Conflict of Interest

The authors declare no conflict of interest.

Author Contributions

Claudia Buerhop-Lutz: Conceptualization (lead); Funding acquisition (lead); Investigation (equal); Methodology (equal); Visualization (equal); Writing—original draft (equal); Writing—review & editing (equal). **Oleksandr Stroyuk**: Investigation (equal); Methodology (equal); Visualization (equal); Writing—original draft (equal); Writing—review & editing (equal). **Oleksandr Mashkov**: Investigation (supporting). **Jens Hauch**: Funding acquisition (supporting). **Ian Marius Peters**: Supervision (lead).

Keywords

anomalies, backsheets, bills of materials, encapsulants, failures, near-infrared absorption spectroscopy, polymer degradation

Received: August 2, 2024
Revised: September 27, 2024
Published online: November 14, 2024

[1] Y. Lyu, A. Fairbrother, M. Gong, J. H. Kim, X. Gu, M. Kempe, S. Julien, K.-T. Wan, S. Napoli, A. Hauser, G. O'Brien, Y. Wang, R. French, L. Bruckman, L. Ji, K. Boyce, *Sol. Energy* **2020**, *199*, 425.
[2] D. Jordan, N. M. Haegel, T. Barnes, *Prog. Energy* **2022**, *4*, 022002.
[3] J. Denz, J. Hepp, C. Buerhop, B. Doll, J. Hauch, C. J. Brabec, I. M. Peters, *Energy Environ. Sci.* **2022**, *15*, 2180.
[4] J. Kim, M. Rabelo, S. P. Padi, H. Yousuf, E.-C. Cho, J. Yi, *Energies* **2021**, *14*, 4278.
[5] A. W. Czanderna, F. J. Pern, *Sol. Energy Mater. Sol. Cells* **1996**, *43*, 101.
[6] D. Sica, O. Malandrino, S. Supino, M. Testa, M. C. Lucchetti, *Renewable Sustainable Energy Rev.* **2018**, *82*, 2934.
[7] C. Buerhop, O. Stroyuk, J. Zöcklein, T. Pickel, J. Hauch, I. M. Peters, *Prog. Photovoltaics: Res. Appl.* **2021**, *30*, 1062.
[8] C. Buerhop, O. Stroyuk, T. Pickel, J. Hauch, I. M. Peters, *Prog. Photovoltaics: Res. Appl.* **2022**, *1–9*, 1161.
[9] L. Koester, S. Lindig, A. Louwen, A. Astigarraga, G. Manzolini, D. Moser, *Renewable Sustainable Energy Rev.* **2022**, *165*, 112616.
[10] W. Luo, Y. S. Khoo, P. Hacke, V. Naumann, D. Lausch, S. P. Harvey, J. P. Singh, J. Chai, Y. Wang, A. G. Aberle, S. Ramakrishna, *Energy Environ. Sci.* **2017**, *10*, 43.
[11] I. Høiaas, K. Grujic, A. G. Imenes, I. Burud, E. Olsen, N. Belbachir, *Renewable Sustainable Energy Rev.* **2022**, *161*, 112353.
[12] M. M. Rahman, I. Khan, K. Alameh, *Renewable Sustainable Energy Rev.* **2021**, *151*, 111532.
[13] W. Herrmann, G. Eder, B. Farnung, G. Friesen, M. Köntges, B. Kubicek, O. Kunz, H. Liu, D. Parlevliet, J. I. A. Tsanakas, J. Vedde, *Qualification of Photovoltaic (PV) Power Plants Using Mobile Test Equipment*, Report IEA-PVPS T13-24:2021 **2021**, ISBN 978-3-907281-12-3.
[14] C. Buerhop, L. Bommes, J. Schlipf, T. Pickel, A. Fladung, I. M. Peters, *Prog. Energy* **2022**, *4*, 042010.
[15] U. Jahn, M. Herz, M. Koentges, D. Parlevliet, M. Paggi, I. Tsanakas, J. Stein, K. Berger, S. Ranta, R. French, M. Richter, T. Tanahashi, in *Review on Infrared and Electroluminescence Imaging for PV Field Application*, International Energy Agency, Paris, France **2018**.
[16] J. A. Tsanakas, L. Ha, C. Buerhop, *Renewable Sustainable Energy Rev.* **2016**, *62*, 695.
[17] O. Kunz, J. Schlipf, A. Fladung, Y. S. Khoo, K. Bedrich, T. Trupke, Z. Hameiri, *Prog. Energy* **2022**, *4*, 042014.
[18] B. Doll, J. Hepp, M. Hoffmann, R. Schüler, C. Buerhop-Lutz, I. M. Peters, J. A. Hauch, A. Maier, C. J. Brabec, *IEEE J. Photovoltaics* **2021**, *11*, 1419.
[19] M. Vuković, I. E. Høiaas, M. Jakovljević, A. S. Flø, E. Olsen, I. Burud, *AIP Conf. Proc.* **2022**, *2487*, 030012.
[20] M. Köntges, A. Morlier, G. Eder, E. Fleiß, B. Kubicek, J. Lin, *IEEE J. Photovoltaics* **2020**, *10*, 616.
[21] D. Colvin, A. Gabor, W. Oltjen, P. Knodle, A. Yao, B. Thompson, N. Khan, S. Lotfian, J. Raby, A. Jojo, X. Yu, M. Liggett, H. Seigneur, R. French, L. Bruckman, M. Li, K. Davis **2024**, https://doi/org/10.36227/techrxiv.171440962.23003014.
[22] C. Buerhop, E. E. van Dyk, F. J. S. Vorster, O. Mashkov, J. L. Crozier McCleland, M. Vumbugwa, J. Hauch, I. M. Peters, *IEEE J. Photovoltaics* **2024**.
[23] C. Buerhop-Lutz, T. Winkler, S. Rupp, M. B. Koentopp, A. Linsenmeyer, B. Jäckel, A. Shirgupe, R. Gottschalg, G. Kleiss, I. M. Peters, in *40th EUPVSEC*, Lisbon, Portugal **2023**.
[24] Electroluminescence (EL) of Photovoltaic Modules – Terms and classification, VDE SPEC 90031 V1.0 **2024**.
[25] O. Stroyuk, C. Buerhop, J. Hauch, I. M. Peters, *Prog. Photovoltaics* **2021**, *30*, 851.
[26] O. Stroyuk, C. Buerhop, E. Wittmann, O. Mashkov, P. Stephan, J. L. Crozier McCleland, M. Vumbugwa, F. J. Vorster, E. E. van Dyk, J. Hauch, C. J. Brabec, I. M. Peters, *Sol. RRL* **2024**, *8*, 2301022.
[27] C. Buerhop, O. Stroyuk, T. Pickel, J. Hauch, I. M. Peters, *Energy Sci. Eng.* **2023**, *11*, 4168.
[28] O. Stroyuk, C. Güttler, C. Buerhop, J. Hauch, I. M. Peters, *ACS Appl. Energy Mater.* **2023**, *6*, 2340.
[29] R. Heidrich, A. Mordvinkin, R. Gottschalg, *Polym. Test.* **2023**, *118*, 107913.
[30] O. Stroyuk, C. Buerhop, A. Vetter, J. A. Hauch, C. J. Brabec, *Sol. Energy Mater. Sol. Cells* **2020**, *216*, 110702.
[31] C. Buerhop, O. Stroyuk, T. Pickel, T. Winkler, J. Hauch, I. M. Peters, *Sol. Energy Mater. Cells* **2021**, *231*, 111295.
[32] A. Morlier, M. Siebert, I. Kunze, G. Mathiak, M. Köntges, *IEEE J. Photovoltaics* **2017**, *7*, 1710.
[33] A. Morlier, F. Haase, M. Köntges, *IEEE J. Photovoltaics* **2015**, *5*, 1735.
[34] B. Doll, E. Wittmann, L. Lüer, J. Hepp, C. Buerhop-Lutz, J. A. Hauch, C. J. Brabec, I. M. Peters, *Phys. Status Solidi RRL* **2023**, *17*, 2300059.
[35] B. Gilleland, W. B. Hobbs, J. B. Richardson, in *2019 IEEE 46th Photovoltaic Specialists Conf. (PVSC)*, Chicago, USA **2019**.
[36] W. B. Hobbs, S. Johnston, B. Gilleland, in *2020 47th IEEE Photovoltaic Specialists Conf. (PVSC)*, Calgary, Canada **2020**.
[37] C. Buerhop, D. Schlegel, M. Niess, C. Vodermayer, R. Weißmann, C. J. Brabec, *Sol. Energy Mater. Sol. Cells* **2012**, *107*, 154.
[38] D. C. Jordan, B. Marion, C. Deline, T. Barnes, M. Bolinger, *Prog. Photovoltaics: Res. Appl.* **2020**, *28*, 739.
[39] L. Bommes, M. Hoffmann, C. Buerhop, J. Hauch, C. J. Brabec, I. M. Peters, *Prog. Photovoltaics: Res. Appl.* **2022**, *30*, 597.

Claudia Buerhop-Lutz has been a Principal Investigator in the area of high-throughput methods for inspecting PV power stations at Helmholtz Institute Erlangen-Nuremberg for Renewable Energy, HI ERN (Forschungszentrum Jülich GmbH) since 2018. She holds a doctoral degree in Material Science (1994) from Friedrich-Alexander University, in Erlangen, Germany. From 2008 to 2018, she headed the group of infrared imaging at the Bavarian Center for Applied Energy Research e.V. in Erlangen, Germany. Dr. Claudia Buerhop-Lutz is the author of more than 120 scientific publications.

Oleksandr Stroyuk is a Research Scientist at Helmholtz Institute Erlangen-Nuremberg for Renewable Energy, HI ERN (Forschungszentrum Jülich GmbH) since 2019. He received his Ph.D. in physical chemistry (2003) and a degree of Doctor of Sciences (2011) from L.V. Pysarzhevsky Institute of Physical Chemistry, National Academy of Sciences of Ukraine. He was a Marie Skłodowska-Curie Fellow at the Technical University of Dresden (2016–2018) and a Research Scientist at the Technical University of Chemnitz (2018–2019). Dr. O. Stroyuk is the author of more than 180 scientific publications.

Oleksandr Mashkov has been a Research Scientist in the High Throughput Characterization and Modelling group at the Helmholtz Institute Erlangen-Nuremberg for Renewable Energy, HI ERN (Forschungszentrum Jülich GmbH) since 2022. He holds a doctoral degree in Material Science and Engineering (2022) from Friedrich-Alexander University in Erlangen, Germany. His professional skills include organic chemistry, electrochromic materials and devices, photochemistry, nanotechnology, and spectroscopic analysis of polymers.

Jens A. Hauch is the head of the research unit for high-throughput methods in photovoltaics at HI ERN (Forschungszentrum Jülich GmbH). He received his Ph.D. in experimental physics from the University of Texas at Austin in 1999. In previous positions, he was Head of the Department of Renewable Energies at the Bavarian Centre for Applied Energy Research (2016–2018), Managing Director of the Energy Campus Nuremberg Research Center until 2015, Managing Director of Konarka Technologies GmbH until 2012, and Senior Scientist at Siemens Corporate Technology. Dr. Hauch is the author of ≈35 patents and more than 80 scientific publications.

Ian Marius Peters heads the group High Throughput Characterization and Modelling at the Helmholtz Institute Erlangen-Nuremberg for Renewable Energy, HI ERN (Forschungszentrum Jülich GmbH) since 2019. He received his Ph.D. in physics (2009) from the Albert Ludwigs University of Freiburg. Previous stations of his career include the Fraunhofer Institute for Solar Energy Systems (ISE), the Solar Energy Research Institute of Singapore (SERIS), and the Massachusetts Institute of Technology (MIT). Dr. I. M. Peters is the author of more than 300 scientific publications.